Improving Dispersion of Multiwalled Carbon Nanotubes in Polyamide 6 Composites Through Amino-Functionalization

Juan Li,[1] Zhengping Fang,[1] Lifang Tong,[1] Aijuan Gu,[1] Fu Liu[2]

[1]*Institute of Polymer Composites, Zhejiang University, Hangzhou 310027, China*
[2]*Institute of Material Physics and Microstructure, Zhejiang University, Hangzhou 310027, China*

Received 26 September 2005; accepted 13 March 2006
DOI 10.1002/app.24599
Published online 9 August 2007 in Wiley InterScience (www.interscience.wiley.com).

ABSTRACT: The focus of this study is to investigate the state of dispersion of different treated multiwalled carbon nanotubes (MWNTs) in polyamide 6 (PA6). The MWNTs used in composites were grafted by 1,6-hexamethylenediamine (HMD) via acid-thionyl chloride to improve their compatibility with PA6 matrix. A microstructure transformation of MWNTs is found during the treatment process. Acidification makes the MWNTs compact and grafting HMD promotes the compact structure loose again. The MWNTs after different treatment were used to fabricate MWNTs/PA6 composites through melt blending. The dispersion of different MWNTs in PA6 was observed by a combination of scanning electron microscopy, optical microscopy, and transmission electron microscopy. The results show that the amino-functionalized MWNTs are dispersed more homogeneously in PA6 than the purified MWNTs, and the poorest dispersion is achieved for acid treated MWNTs. It is indicated that the loose structure and functionalized surface of MWNTs benefit the dispersion of MWNTs in PA6. In addition, the amino-functionalization of MWNTs improves the compatibility between the MWNTs and PA6, resulting in stronger interfacial adhesion. © 2007 Wiley Periodicals, Inc. J Appl Polym Sci 106: 2898–2906, 2007

Key words: amino-functionalization; carbon nanotubes; polyamide 6; composites; dispersions

INTRODUCTION

Carbon nanotubes (CNTs) are potentially excellent mechanical reinforcing fillers in polymer composites.[1–8] Although the properties of CNTs are remarkable, the surface area of these tubes in nanoscale is so large that they tend to form aggregation, which is disadvantageous for homogeneous dispersion of CNTs in polymer. Usually when some impurities are present in a certain material, they would become stress concentration points, which will initiate the cracks. If the aggregation of CNTs is formed in the polymer matrix, they may act as the stress concentration points, thus affecting the mechanical properties of a given composition directly.[9] On the other hand, the surface of nanotubes is slippery and nonpolar. The interfacial adhesion between CNTs and polymer matrix is usually poor. The stress transfer from the matrix to the reinforcement depend on a strong interfacial strength.[10–12] So the dispersion of CNTs in polymer and the interfacial adhesion between CNTs and polymer are the most important challenges in the development of high-performance CNTs/polymer composites.

Correspondence to: L. Tong (zpfang@zju.edu.cn).

Journal of Applied Polymer Science, Vol. 106, 2898–2906 (2007)

Many methods have been adopted to address abovementioned questions, including noncovalent surfactant,[13] polymer-wrapping,[14] and covalent functionalization using open-end and sidewall chemistry.[15–17] The covalent functionalization of MWNTs is considered as one of the most effective means for homogeneous dispersion of carbon nanotubes in solution and polymer. Some small molecules such as alkyl ethanol,[18] alkylamine,[19] and even polymer chains, including polystyrene,[20] poly(ethylene glycol),[21] poly(vinyl alcohol),[22] have been grafted onto CNTs. For example, Mitchell et al.[23] prepared polystyrene composites with purified and organically modified single-walled carbon nanotubes (SWNTs) by solution mixing. An improved compatibility between SWNTs and polymer and a better dispersion of SWNTs in the polymer are obtained. Gojny and his colleagues[24] fabricated epoxy composites with multiwalled carbon nanotubes (MWNTs) grafted by multifunctional amine. They discovered that the functionalization of MWNTs led to a reduced agglomeration and improved interaction between the nanotubes and the epoxy resin. Lin et al.[22] fabricated poly(vinyl alcohol)/CNTs composites film. They found that grafting polymer onto CNTs is an effective approach for the homogeneous dispersion of CNTs in the polymer matrix.

Polyamide 6 (PA6) is a typical semicrystalline thermoplastic with a wide range of engineering applications

because of its attractive combination of good processibility, mechanical properties, and chemical resistance. Fabricating MWNTs/PA6 composites has received increasing interest.[25–27] The poor compatibility between the polar PA6 and the nonpolar MWNTs make uniform dispersion of MWNTs into PA6 difficult. The surface modification of MWNTs becomes especially important for homogeneous dispersion of MWNTs in PA6. In the previous researches, the acid treatment was often used to increase the polarity of MWNTs and enhance the compatibility between MWNTs and PA6.[26,27] However, few study was focused on the modification of MWNTs by other functional groups. It is necessary to find a new and better modified method to promote the dispersion of MWNTs in PA6 and improve the interfacial adhesion between MWNTs and PA6. Considering the molecular structure of PA6 itself, 1,6-hexamethylenediamine (HMD), a monomer of polyamide, is selected to modify the surface characteristics of MWNTs.

In our previous work,[28] it has been proven that the HMD can be covalently grafted onto MWNTs successfully. In this study, the MWNTs after different treatment were used to fabricate MWNTs/PA6 composites via melt-blending. The aim was to investigate the effect of different treatment on the dispersion of MWNTs in PA6 matrix. For this purpose, optical microscope (OM), scanning electron microscope (SEM), and transmission electron microscope (TEM) were used to observe the dispersion state of MWNTs in PA6.

EXPERIMENTAL

Materials

MWNTs were synthesized by chemical vapor deposition (CVD) technique from acetylene at 700°C for 60 min. The pristine MWNTs were purified through soaking in concentrated nitric acid 48 h at room temperature. PA6 pellets (Grade CM 1017 from Toray, Japan) was used in this experiment.

Functionalization of MWNTs

Amine-functionalized MWNTs (f-MWNTs) were prepared via acid-thionyl chloride road, as shown in Figure 1.

The purified MWNTs (*p*-MWNTs) were mixed with sulfuric (98%) and nitric (68%) acid (3 : 1 in volume) and treated in ultrasonic bath at 50°C for 4 h. The excess acid was washed thoroughly with deionized water until the pH value of water was about 7. The acid-treated MWNTs (a-MWNTs) were dried at 80°C in a vacuum oven overnight and then grinded into powder with a carnelian mortar. The mixture of a-MWNTs, thionyl chloride ($SOCl_2$), and *N*,*N*-dimethylformamide (DMF) (a typical ratio of MWNTs: $SOCl_2$: DMF is 100 mg : 20 mL : 1 mL) was treated in a ultrasonic bath for about 2 h and then refluxed at 70°C for 24 h. Then, $SOCl_2$ was removed by distillation and the remained black solid was dried at room temperature under vacuum. The gained solid was reacted with excess HMD at 120°C for 72 h. After washing the MWNTs with anhydrous ethanol repeatedly, the HMD was removed and the resulting amino-functionalized MWNTs (f-MWNTs) were dried under vacuum.

Preparation of MWNTs/PA6 composites

The PA6 pellets and MWNTs were dried under vacuum at 80°C for 24 h before extruding. The PA6 composites with MWNTs content from 0.1 to 1.0 wt % were prepared via a melt-blending method using a PRISM TSE-16-TC Brabender twin-screw extruder. The barrel temperature, from the entrance to the exit, was 185, 228, 235, 235, and 225°C, respectively. The rotation speed of the twin screw was maintained 30 rpm.

Characterization

A SEM (HITACHIS-570) was used to investigate the surface morphology of composites products after extruding. A field emission scanning electron microscope (FESEM, SIRION FEI, USA) was used to observe the morphology of MWNTs and the fracture surfaces of the MWNTs/PA6 composites after tensile tests. A XP-203 OM, product of Changfang Optical Instrument Co., Shanghai, China, with CCD camera was used to study the dispersion of various MWNTs in PA6. The samples were compressed into film with thickness of $\sim$ 100 μm. TEM observation of the dispersion of different MWNTs in the PA6 matrix was performed with a JEM 1230 TEM instrument operated under an acceleration voltage of 300 kV. The sections are about 50–150 nm in thickness prepared by ultramicrotome cutting at room temperature.

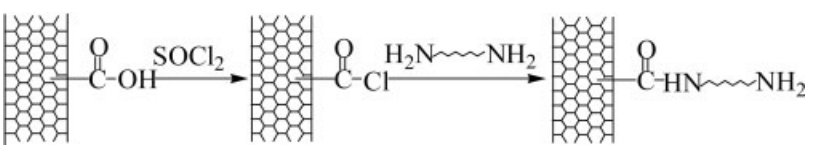

Figure 1 Schematic representation of the procedure for the formation of f-MWNTs.

RESULTS AND DISCUSSION

Morphology of MWNTs

FESEM images of *p*-MWNTs, a-MWNTs, and f-MWNTs are shown in Figure 2. It is clear that the stacking behavior of the three kinds of MWNTs is different. The *p*-MWNTs in Figures 2(a.1) and 2(a.2) are randomly and loosely entangled together. However, the a-MWNTs are compact and massive, which is different from the *p*-MWNTs obviously. In Figure 2(b.1),

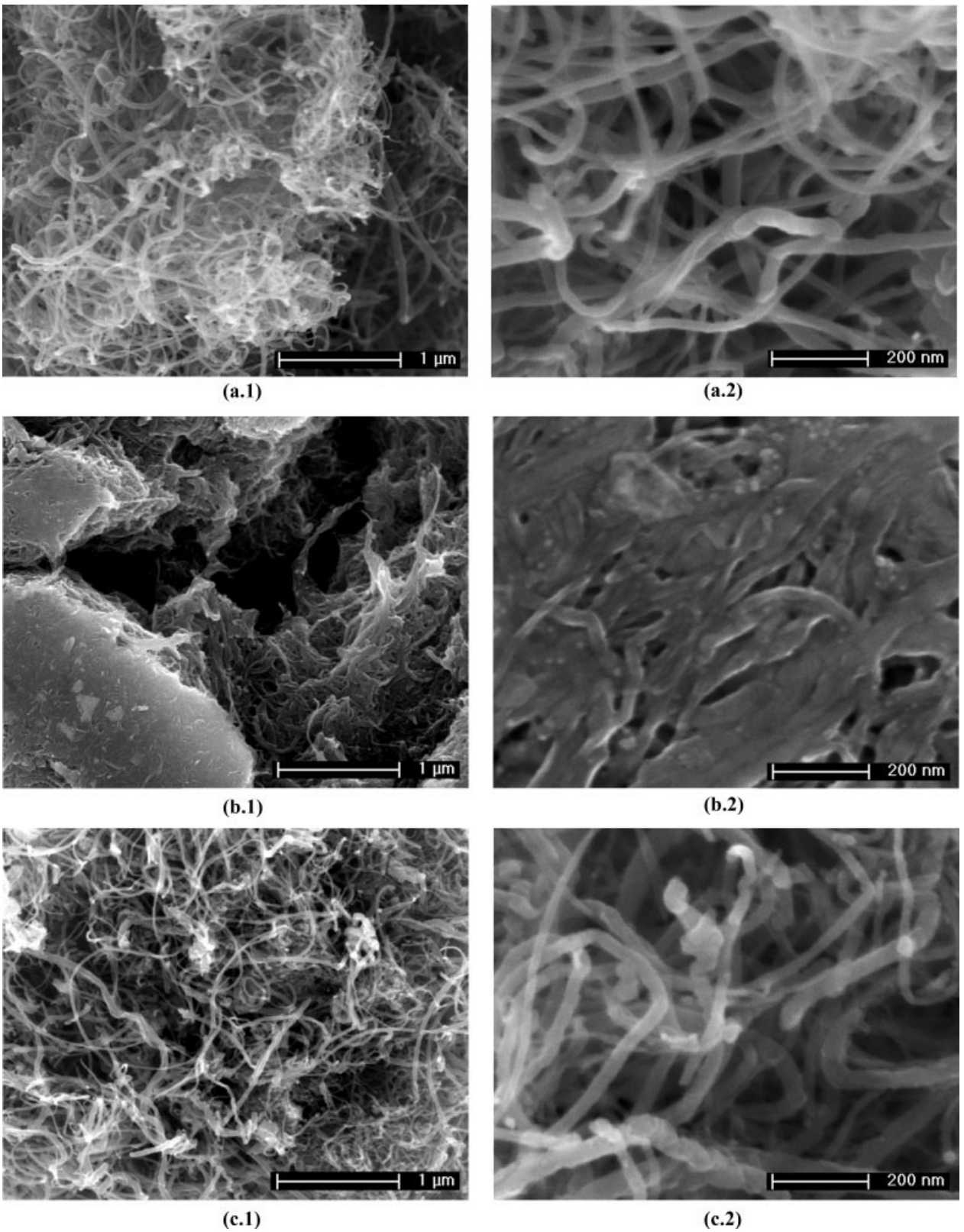

Figure 2 FESEM images of (a.1,a.2) *p*-MWNTs, (b.1,b.2) a-MWNTs, (c.1,c.2) f-MWNTs.

a conglomeration of a-MWNTs can be observed. Under higher magnification, it is found that some tubes are adhered together and almost no interspace remains in the conglomerated tubes as denoted by the arrow in Figure 2(b.2). After grafting HMD, these tubes stacks loosely again as shown in Figures 2(c.1) and 2(c.2). The change of microstructure transformation of MWNTs usually causes different apparent volume of MWNTs. Figure 3 shows the state of different MWNTs in bottles with the same mass (100 mg). The volume of *p*-MWNTs is larger than a-MWNTs and the largest volume is obtained for f-MWNTs. This change indicates that acidification makes the MWNTs compact and grafting HMD promotes the compact structure loose again.

Dispersion of MWNTs in PA6

The dispersion of MWNTs in polymer matrix is one of the most important questions for fabricating high-performance MWNTs/polymer composites. However, characterization and quantification the state of MWNTs dispersion in polymer is a difficult task. Direct microscopic observation is difficult to apply due to the extreme differences in radial and axial dimensions of the nanotubes. SEM can be used to observe the interfacial morphology of the composites. OM can be used to observe big agglomerates of nanotubes but is incapable to analyze the dispersion of single tube at the microcosmic scale. TEM on thin section has the advantage of showing all segments of nanotubes located within the thickness of the section; however, it is difficult to get an entire state of dispersion of the system. Therefore, in this study, the combination of abovementioned three methods is adopted to observe the dispersion of MWNTs in PA6 clearly.

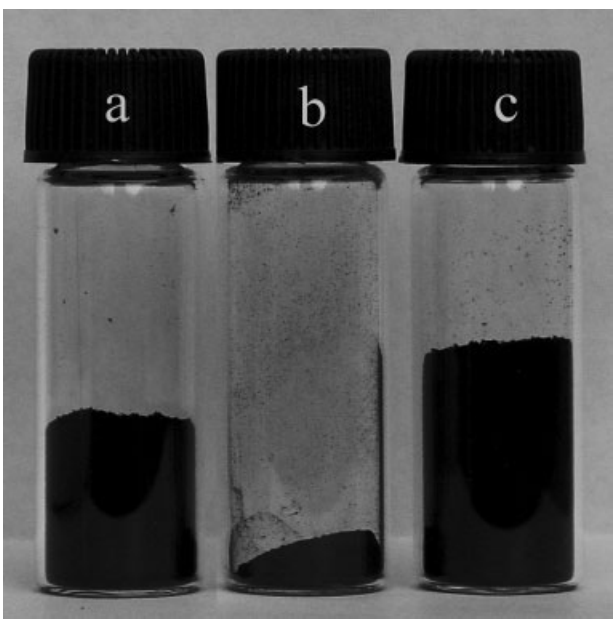

Figure 3 Observation of apparent volume change for (a) *p*-MWNTs, (b) a-MWNTs, (c) f-MWNTs with the same mass (100 mg).

The direct evidence for the dispersion of various MWNTs in PA6 is the darkness of the composites. All the *p*-MWNTs/PA6 composites are black irrespective of the MWNTs concentration increasing from 0.1 to 1.0 wt %. However, the f-MWNTs/PA6 composites changes from light to deep gray with the increasing MWNTs concentration. This phenomenon reflects different dispersion behavior of MWNTs in the composites. Figure 4 shows the surface morphology of extruded products containing 1.0 wt % MWNTs. The surfaces of *p*-MWNTs/PA6 [Figs. 4 (a.1) and 4(a.2)] and f-MWNTs/PA6 [Figs. 4(c.1) and 4(c.2)] composites are both smooth, but the surfaces of a-MWNTs/PA6 [Figs. 4(b.1) and 4(b.2)] composite are very coarse. Some large heave and groove can be found in a-MWNTs/PA6 composites under higher magnification in Figure 4(b.2). This is connected with the different dispersion of MWNTs in PA6. When the extruded product is pulled into thin fiber, even some large carbon blocks in PA6 can be found in a-MWNTs/PA6 composites. The results indicate the loose structure benefits the dispersion of MWNTs in PA6. The strong interaction in a-MWNTs makes the compact a-MWNTs blocks hard to be dispersed by during extruding process. For *p*-MWNTs/PA6 and f-MWNTs/PA6 composites, their surfaces are both smooth. It is difficult to observe the difference between them from Figure 4. Then OM was used to observe the dispersion of MWNTs in PA6.

Figure 5 shows the OM images of MWNTs/PA6 composites with different magnification. Obviously, the whole dispersion of *p*-MWNTs in PA6 is homogeneous under lower magnification; few large aggregations can be found. However, under higher magnification, some aggregations of MWNTs and large area without MWNTs can be found suggesting the poor dispersion. In both Figures 5(b.1) and 5(b.2), many large a-MWNTs agglomerations are observed in the composite, which indicates the compact a-MWNTs blocks are not be dispersed during melt-blending. This is in agreement with earlier analysis. For f-MWNTs/PA6 composite, the size and amount of f-MWNTs aggregations in the composites are much less than *p*-MWNTs/PA6 composite. The results indicate that the functionalization of MWNTs increase the dispersion of MWNTs in PA6 matrix.

Figure 6 shows the TEM images of the *p*-MWNTs/PA6 and f-MWNTs/PA6 composites. The nanotubes in single [Figs. 6(a.2) and 6(b.2)] and aggregate [Figs. 6(a.1) and 6(b.1)] are both found in two composites. But it is easier to find more and larger aggregations of MWNTs in *p*-MWNTs/PA6 composites than in f-MWNTs/PA6 composites. Moreover, the amount of f-MWNTs in MWNTs enriched

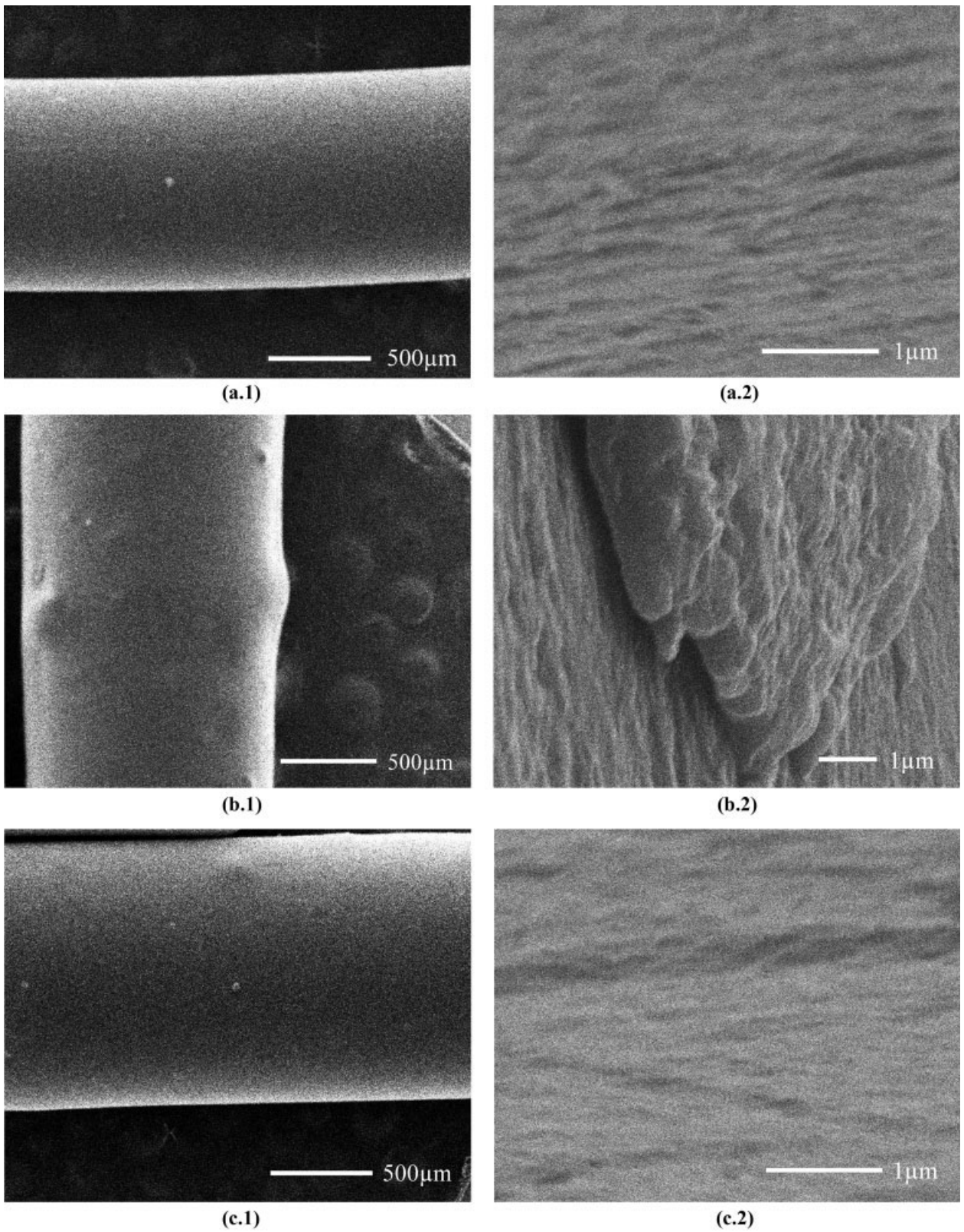

Figure 4 SEM images showing the surface morphology of (a.1,a.2) *p*-MWNTs/PA6, (b.1,b.2) a-MWNTs/PA6, and (c.1,c.2) f-MWNTs/PA6 composites after extruding with 1.0 wt % MWNTs.

domain is fewer than that of *p*-MWNTs. Although the f-MWNTs are not dispersed in single tube homogeneously, the dispersion of MWNTs has been improved significantly. Combining of SEM, OM, and TEM observation, it is believed that the f-MWNTs obtain better dispersion in PA6.

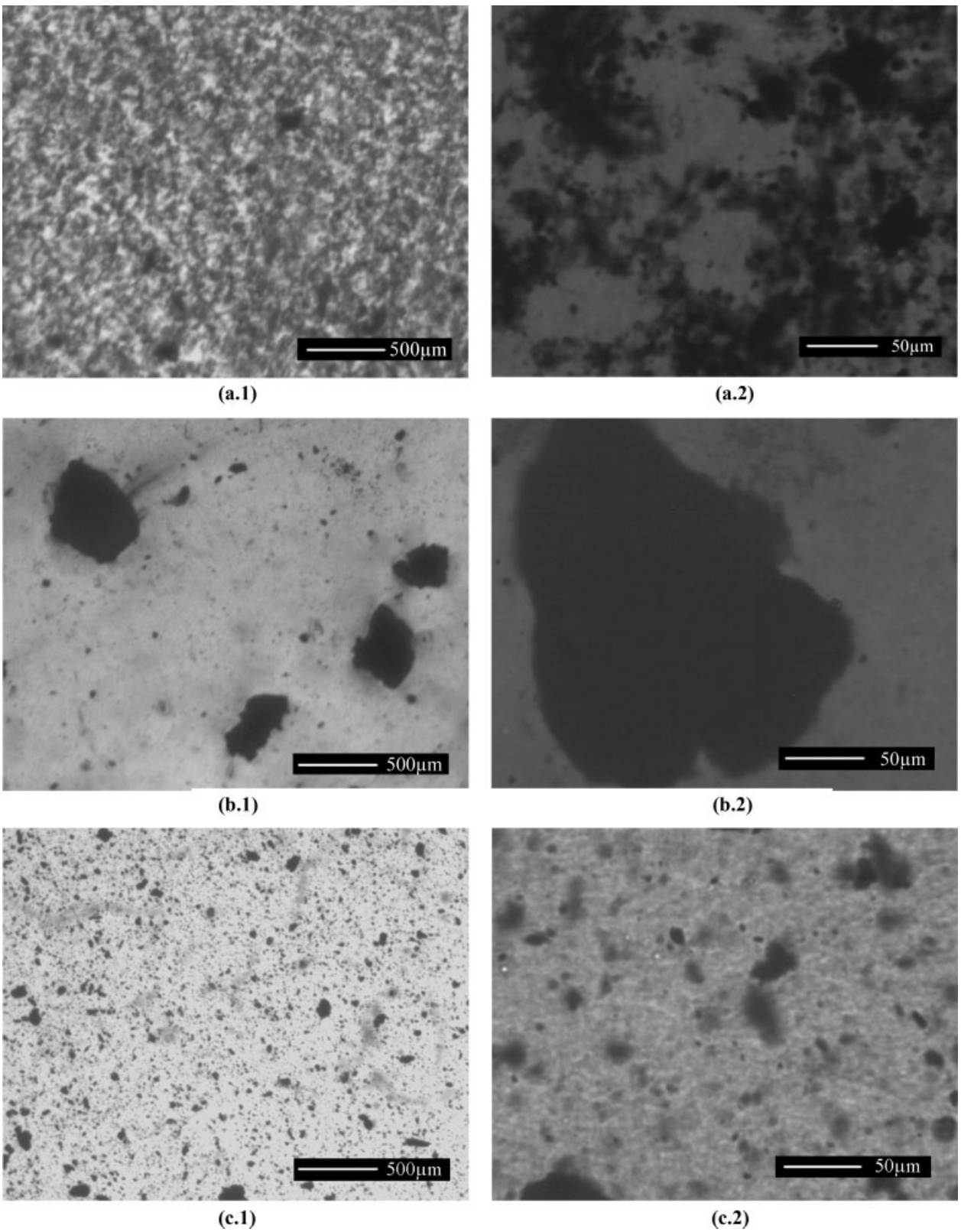

Figure 5 OM images showing the dispersion of 1.0 wt % (a.1,a.2) *p*-MWNTs, (b.1,b.2) a-MWNTs, and (c.1,c.2) f-MWNTs in PA6 matrix.

The interface between MWNTs and PA6 may be the foremost factors for the different dispersion of MWNTs in PA6. It is well-known that the dispersion of MWNTs in resin is divided into two steps usually. First, MWNTs networks are wetted by the resin molecules; second, the individual tubes diffuse into the

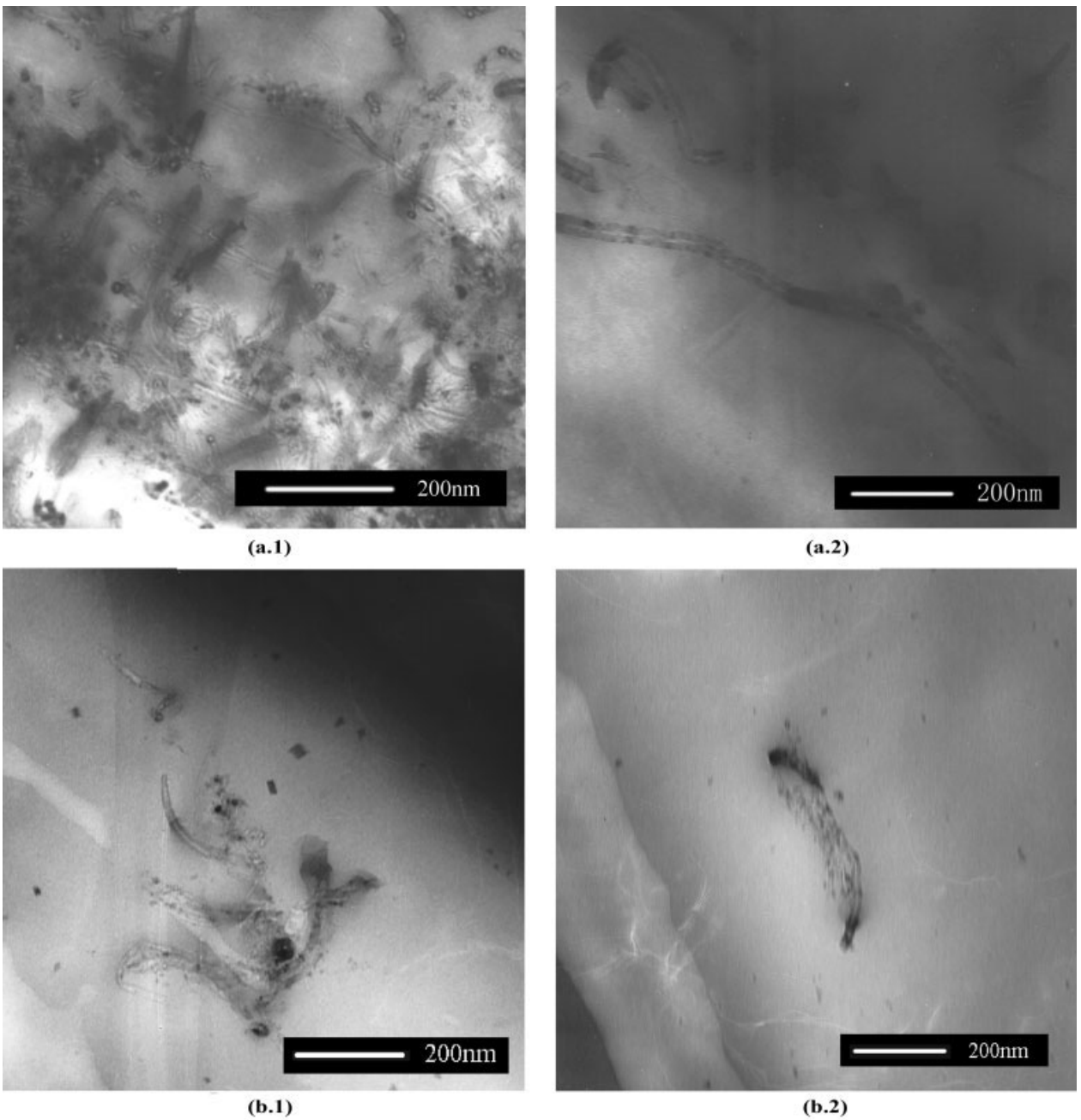

Figure 6 TEM images showing the dispersion of 1.0 wt % (a.1,a.2) *p*-MWNTs and (b.1,b.2) f-MWNTs in PA6 composites.

matrix uniformly. The compatibility between *p*-MWNTs and PA6 is poor, and so these *p*-MWNTs can only be wetted forcedly during extruding. It is difficult for them to diffuse into PA6 further. Therefore, the *p*-MWNTs can only be dispersed in loose aggregations of tubes in PA6. Acid treatment improves the polarity of MWNTs and makes them be wetted by PA6 more easily, but the interaction in a-MWNTs is stronger than that between a-MWNTs and PA6. The inside of the a-MWNTs agglomeration cannot be wetted. Thus, it is difficult for the individual tube to diffuse into PA6 in the limited time during melt-extruding. By grafting HMD, the compact structure is broken, and the MWNTs become loosely again. Furthermore, the compatibility between f-MWNTs and matrix is better than *p*-MWNTs. Therefore, these tubes are more easily to be wetted and diffuse into the matrix, which results in more homogeneous dispersion of f-MWNTs in PA6.

Morphology of the fracture surface of composites

Figure 7 shows the SEM images of the fracture surfaces for *p*-MWNTs/PA6 and f-MWNTs/PA6 composites. As shown in the OM and TEM images, in both composites, some aggregations of MWNTs can be observed. But more aggregations of MWNTs are

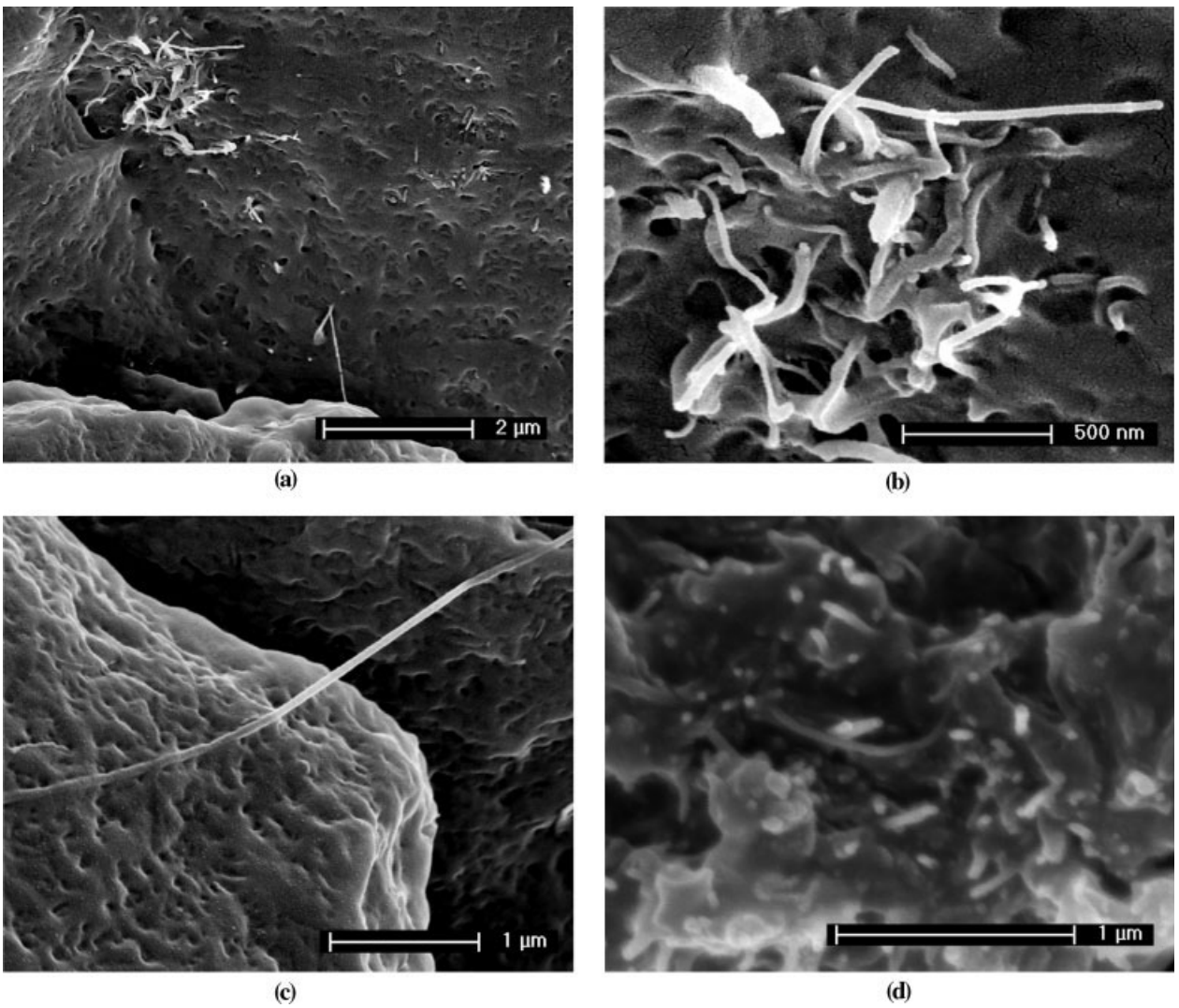

Figure 7 FESEM images showing the fracture surface of (a,b,c) *p*-MWNTs/PA6 and (d) f-MWNTs/PA6 composites with 1.0 wt % MWNTs.

found in *p*-MWNTs/PA6 composites. Magnifying an aggregation of *p*-MWNTs in Figure 7(b), we can see that many long tubes are pulled out and some holes exist in the spot where MWNTs embedded in the matrix. Moreover, a tube several tens in length lying on the fracture surface can be observed in Figure 7(c), with some sections embedded by PA6 and others debonded. The behavior means a poor wetting and imperfect interfacial adhesion between *p*-MWNTs and the polymer matrix. For f-MWNTs/PA6 composites, few MWNTs are pulled out, which suggests a better wettability and more perfect interfacial adhesion of f-MWNTs by the PA6 matrix.

CONCLUSIONS

HMD was grafted onto MWNTs via acid-thionyl chloride to improve the compatibility between MWNTs and PA6. It is found that the acid treatment makes the MWNTs compact and grafting HMD results in a more loose structure than the pristine one. The state of dispersion of MWNTs after different treatment in PA6 matrix was studied. The results show that a better dispersion is obtained for *p*-MWNTs than a-MWNTs and the best dispersion is observed for f-MWNTs. It is indicated that loose stacking and amino-functionalized surface of MWNTs benefit the dispersion of MWNTs in PA6. In addition, the SEM observation of the fracture surface of the composite suggests that grafting HMD improves the interfacial adhesion between MWNTs and PA6.

References

1. Thostenson, E. T.; Ren, Z. F.; Chou, T. W. Compos Sci Technol 2001, 61, 1899.
2. Andrews, R.; Weisenberger, M. C. Curr Opin Solid State Mater Sci 2004, 8, 31.

3. Lau, K. T.; Hui, D. Compos B 2002, 35, 263.
4. Shaffer, M. S. P.; Windle A. H. Adv Mater 1999, 11, 937.
5. Jin, Z. X.; Pramoda, K. P.; Xu, G. Q.; Goh, S. H. Chem Phys Lett 2001, 337, 43.
6. Bhattacharyya, A. R.; Pötschke, P.; Abdel-Goad, M.; Fischer, D. Chem Phys Lett 2004, 392, 28.
7. Zou, Y. B.; Feng, Y. C.; Wang, L.; Liu, X. B. Carbon 2004, 42, 271.
8. Goh, H. W.; Goh, S. H.; Xu, G. Q.; Pramoda, K. P.; Zhang, W. D. Chem Phys Lett 2003, 373, 277.
9. Ptschke, P.; Bhattacharyya, A. R.; Janke, A. Eur Polym J 2004, 40, 137.
10. Barber, A. H.; Cohen, S. R.; Kenig, S.; Wagner, H. D. Compos Sci Technol 2004, 64, 2283.
11. Qian, D.; Liu, W. K.; Ruoff, R. S. Compos Sci Technol 2003, 63, 1561.
12. Lau, K. T. Chem Phys Lett 2003, 370, 399.
13. Shaffer, M. S. P.; Fan, X.; Windle, A. H. Carbon 1998, 36, 1603.
14. O'connell, M. J.; Boul, P.; Ericson, L. M.; Huffman, C.; Wang, Y.; Haroz, E.; Kuper, C.; Tour, J.; Ausman, K. D.; Smalley, R. E. Chem Phys Lett 2001, 342, 265.
15. Tasis, D.; Tagmatarchis, N.; Georgakilas, V.; Prato, M. Chem Eur J 2003, 9, 4000.
16. Sun, Y. P.; Fu, K. F.; Lin, Y.; Huang, W. J. Acc Chem Res 2002, 35, 1096.
17. Dyke, C. A.; Tour, J. M. Chem Eur J 2004, 10, 812.
18. Hamon, M. A.; Hui, H.; Bhowmik, P.; Itkis, H. M. E.; Haddon, R. C. Appl Phys A 2002, 74, 333.
19. Stevens, J. L.; Huang, A. Y.; Peng, H. Q.; Chlang, I. W.; Khabashesku, V. N.; Margrave, J. L. Nano Lett 2003, 3, 331.
20. Hill, D. E.; Rao, A. M.; Allard, L. F.; Sun, Y. P. Macromolecules 2002, 35, 9466.
21. Huang, W. J.; Fernando, S.; Allard, L. F.; Sun, Y. P. Nano Lett 2003, 3, 565.
22. Lin, Y.; Zhou, B.; Fernando, K. A. S.; Liu, P.; Allard, L. F.; Sun, Y.-P. Macromolecules 2003, 36, 7199.
23. Mitchell, C. A.; Bahr, J. L.; Arepalli, S.; Tour, J. M.; Krishnamoorti, R. Macromolecules 2002, 35, 8825.
24. Gojny F. H.; Nastalczyk, J.; Roslaniec, Z.; Schulte K. Chem Phys Lett 2003, 370, 820.
25. Xia, H. S.; Wang, Q.; Qiu, G. H. Chem Mater 2003, 15, 3879.
26. Zhang, W. D.; Shen, L.; Phang, I.; Liu, T. Macromolecules 2004, 37, 256.
27. Liu, T. X.; Phang, I. Y.; Shen, L.; Chow, S. Y.; Zhang, W. D. Macromolecules 2004, 37, 7214.
28. Li, J.; Fang, Z. P.; Tong, L. F.; Gu, A. J.; Liu, F. Acta Phys Chim Sin 2005, 21, 1244.